

Lower sensitivity to peripheral hypermetropic defocus due to higher order ocular aberrations

Petros Papadogiannis , Dmitry Romashchenko, Peter Unsbo and Linda Lundström

Department of Applied Physics, Royal Institute of Technology (KTH), Stockholm, Sweden

Citation information: Papadogiannis P, Romashchenko D, Unsbo P & Lundström L. Lower sensitivity to peripheral hypermetropic defocus due to higher order ocular aberrations. *Ophthalmic Physiol Opt* 2020. <https://doi.org/10.1111/opo.12673>

Keywords: peripheral vision, asymmetry, defocus, myopia

Correspondence: Petros Papadogiannis
E-mail address: petrospa@kth.se

Received: 9 September 2019; Accepted:
7 January 2020

Author contributions: PP and LL: involved in all aspects of study conception and design; data acquisition, analysis and interpretation; and drafting and critically revising the manuscript. DR: involved in data acquisition, analysis and interpretation; and critically revising the manuscript. PU: involved in study design and critically revising the manuscript.

Abstract

Purpose: Many myopia control interventions are designed to induce myopic relative peripheral refraction. However, myopes tend to show asymmetries in their sensitivity to defocus, seeing better with hypermetropic rather than myopic defocus. This study aims to determine the influence of chromatic aberrations (CA) and higher-order monochromatic aberrations (HOA) in the peripheral asymmetry to defocus.

Methods: Peripheral (20° nasal visual field) low-contrast (10%) resolution acuity of nine subjects (four myopes, four emmetropes, one hypermetrope) was evaluated under induced myopic and hypermetropic defocus between ± 5 D, under four conditions: (a) Peripheral Best Sphere and Cylinder (BSC) correction in white light; (b) Peripheral BSC correction + CA elimination (green light); (c) Peripheral BSC correction + HOA correction in white light; and (d) Peripheral BSC correction + CA elimination + HOA correction. No cycloplegia was used, and all measurements were repeated three times.

Results: The slopes of the peripheral acuity as a function of positive and negative defocus differed, especially when the natural HOA and CA were present. This asymmetry was quantified as the average of the absolute sum of positive and negative defocus slopes for all subjects (AVS). The AVS was 0.081 and 0.063 logMAR/D for white and green light respectively, when the ocular HOA were present. With adaptive optics correction for HOA, the asymmetry reduced to 0.021 logMAR/D for white and 0.031 logMAR/D for green light, mainly because the sensitivity to hypermetropic defocus increased when HOA were corrected.

Conclusion: The asymmetry was only slightly affected by the elimination of the CA of the eye, whereas adaptive optics correction for HOA reduced the asymmetry. The HOA mainly affected the sensitivity to hypermetropic defocus.

Introduction

The overall aim of this research is to unravel the cues for the visual regulation of ocular growth and the ability of the peripheral retina to detect the sign of defocus. Knowledge of ocular growth regulation is of key interest for myopia prevention, as myopia most often arises because the eye grows too long in relation to its optical power. Today the prevalence of myopia is increasing rapidly. In a recent report regarding global myopia trends, the World Health Organization (WHO) estimated that by 2050 half of the world's population will be myopic.¹ Since myopes face a

greater risk of developing retinal detachment and glaucoma, which can lead to blindness,² WHO concludes that it is important to halt the progression of myopia.

The increasing prevalence of myopia is most likely due to changes in the visual environment, with increasing near-work and less time spent outdoors.^{3,4} A visual regulation of ocular growth means that the retina is able to detect the sign of defocus, i.e. that it can differentiate between myopic (positive) defocus, supposedly providing a stop signal to further growth, and hypermetropic (negative) defocus, supposedly leading to continued growth. Furthermore, animal studies have shown that the peripheral parts of the retina

can be more related to growth regulation than the fovea.^{5,6} Studies on several different species have shown that the peripheral retina can slow or accelerate ocular growth depending on the sign of the peripheral refraction. It is believed that peripheral image quality is linked to ocular growth and myopia also in humans.⁷ Today, many optical myopia intervention techniques are therefore designed to induce myopic defocus on the peripheral retina.⁸ However, their success varies and we need to identify the protective optical properties to optimise the optical design of these corrections.

Little is known of how the ocular growth regulation system detects the sign of defocus. This study tests two hypotheses based on the assumption that there are optical asymmetries in the image quality on the peripheral retina that can be detected via psychophysical evaluation, i.e. that a different visual response to the sign of defocus on cortical level originates from the same visual input as the signal for growth regulation on a retinal level. Peripheral vision is a complex mixture of optical limitations and low neural sampling⁹; although the limiting factor for peripheral high-contrast resolution is neural, high-contrast detection and low-contrast resolution depend on optical image quality.^{10–14} Visual performance has indeed been found to show asymmetric response to the sign of defocus both centrally and in the periphery; both Guo *et al.* and Radhakrishnan *et al.* found asymmetries to the sign of defocus in the fovea,^{15,16} and Rosén *et al.* showed that negative defocus i.e. when the image is located behind the retina, affects peripheral visual acuity less in myopes than in emmetropes.^{14,17} The latter study hypothesised that the asymmetric sensitivity to defocus in low-contrast resolution is caused by the ocular higher-order monochromatic aberrations (HOA).¹⁷ However, the large chromatic aberrations (CA) of the eye also provide cues to the sign of defocus, and ocular growth in chickens can be induced through manipulating longitudinal chromatic aberration.¹⁸ In the human eye, longitudinal chromatic aberration does not vary considerably across the visual field,^{19,20} but both transverse CA and HOA increase with eccentricity.^{21,22} It is thereby possible that asymmetric optical aberrations, such as coma and chromatic aberration, produce an asymmetric depth of focus that provides the peripheral retina with cues to the sign of defocus. Therefore, the aim of this study is to elucidate the role of CA and HOA in the response to peripheral defocus.

This article evaluates the variation in peripheral vision for different signs and magnitudes of defocus with and without aberrations present under well-controlled conditions. Our null hypotheses are: (1) the asymmetric sensitivity to the sign of defocus is not affected by the CA of the eye and (2) the asymmetry is not affected by the HOA of the eye. The results show that the second hypothesis can be rejected.

Methods

Nine subjects with good general and ocular health, aged between 25 and 47 years, participated in this study. According to their habitual refraction, the subject group consisted of four emmetropes, four myopes (foveal refraction ranging from -1 D to -2.5 D), and one hypermetrope ($+1$ D) and is presented in more detail in Table 2. All nine participants were evaluated for their peripheral low-contrast resolution acuity thresholds under induced positive (myopic) and negative (hypermetropic) defocus between ± 5 D in white and green (monochromatic) light. The experiment was performed under four conditions of peripheral optical correction (also summarised in Table 1):

- a) Peripheral Best Sphere and Cylinder (BSC) correction in white light,
- b) Peripheral BSC correction + CA elimination (green light),
- c) Peripheral BSC correction + HOA correction in white light and
- d) Peripheral BSC correction + CA elimination + HOA correction.

Acuity thresholds and wavefront aberrations were measured in the 20° nasal visual field of the subject's right eye with natural pupil sizes, and the left eye was used for fixation on a Maltese cross mounted 2.6 m away. A chin-forehead-rest was used for stability. Throughout the experiment, the fixation was monitored by an infrared camera and a Hartmann-Shack (HS) sensor, and the subjects were realigned if necessary. The study was approved by the regional ethics committee, the tenets of the Declaration of Helsinki were followed, and informed consent was given by the subjects prior to participation.

A laboratory-based adaptive optics (AO) system running in continuous closed loop was used for peripheral HOA correction. The system operates in near-infrared light (830 nm) and consists of the miraoTM 52 D deformable mirror (52 actuators, ± 50 μ m stroke, corrects up to sixth Zernike order) and the HASOTM wavefront sensor; both components are from imagine eyes (www.imagine-eyes.com). The system is calibrated for measurements in visible light and has been previously described by Rosén *et al.*²³ To

Table 1. The different conditions of peripheral correction (explained in the methods section) under which the experiments were performed

	White stimuli	Green stimuli (CA elimination)
Refractive correction	a) Peripheral BSC correction	b) Peripheral BSC correction
Refractive + Adaptive optics correction	c) Peripheral BSC + HOA correction	d) Peripheral BSC + HOA correction

Each condition is represented by one colour. The same colours are used for the same conditions in Figure 1. (BSC-Best Sphere and Cylinder, HOA-Higher Order Aberrations, CA-Chromatic Aberration)

measure the peripheral lower- and higher-order aberrations, the same AO system was used, but now with the deformable mirror set to static compensation only for the internal aberrations of the AO system. Peripheral BSC at 20° nasal visual field were corrected by trial lenses, which were placed on a trial lens holder aligned with the field angle in front of the subject's right eye. The peripheral correction for the refractive errors was calculated from the corresponding second-order Zernike coefficients, which were extracted from the off-axis wavefront measurements and converted into dioptres using the following formulas²⁴:

$$M = -\frac{4\sqrt{3}}{r_{pupil}^2}c_2^0, \quad J0 = -\frac{2\sqrt{6}}{r_{pupil}^2}c_2^2,$$

$$J45 = -\frac{2\sqrt{6}}{r_{pupil}^2}c_2^{-2},$$

$$\text{Cylinder} = -2\sqrt{(J0^2 + J45^2)},$$

$$\text{Sphere} = M - \left(\frac{\text{cylinder}}{2}\right) \text{ and}$$

$$\text{axis} = 0.5 * \text{atan}\left[\frac{J45}{J0}\right]$$

where c_n^m is the corresponding Zernike coefficient and r_{pupil} is the radius of the pupil.

After the trial lenses were placed in the holder, the state of the peripheral correction was checked by wavefront measurements. If the peripheral correction was not adequate, the trial lenses were adjusted in 0.25 D steps until the wavefront data showed full peripheral refractive correction. For CA elimination (green/monochromatic light conditions), a narrow band pass filter (550 nm; bandwidth 25 nm) was placed in the path between the visual stimuli presentation screen and the AO system, in a similar manner as in a recent publication from Venkataraman *et al.*²⁵ The average luminance was kept at 24 cd/m² for both white and green (monochromatic) light conditions.

Positive and negative defocus between ±5 D (in five steps) was induced in random order by changing the spherical power of the trial lens correction of each subject (i.e. for a -1 D myopic subject in the periphery, the -1 D corrective trial lens was substituted by a +1 D trial lens in order to obtain an induced defocus value of +2 D). When the AO system was running in a closed loop, the deformable mirror was set to target for the desired defocus value while it was correcting for the HOA and any residual astigmatism. No cycloplegia was used to control the state of accommodation. The HS wavefront sensor in the AO system therefore recorded the pupil size and peripheral

wavefront data live during the experiment to take any changes in accommodation into consideration. The Zernike coefficients were expressed over an inscribed circle in the natural elliptical pupil and converted into dioptres of defocus using the following formula²⁶:

$$M = \frac{4\sqrt{3}}{r_{pupil}^2}c_2^0 + \frac{12\sqrt{5}}{r_{pupil}^2}c_4^0$$

The effect on the Zernike coefficients of ignoring the elliptical shape of the natural pupil is minor at 20° off-axis²⁷, and did not affect the state of the HOA correction. The spectacle magnification, determined from the power of the trial lens and the vertex distance, was taken into consideration to achieve the actual off-axis defocus that the eye was experiencing in the plane of the entrance pupil. Finally, this defocus was averaged over time for each condition and subject. The size of the displayed gratings was also adjusted to compensate for the spectacle magnification to avoid any artefacts in the reported acuity values due to different trial lens powers.

All subjects were evaluated for their peripheral resolution acuity in low contrast, since this task is limited by the optical properties and not by neural sampling.^{13,14} Low-contrast (10%) Gabor gratings in a Gaussian window with a standard deviation of 1.6° were used as a stimulus pattern.^{23,25} The gratings had an oblique orientation (-45° and 45°) in order to avoid any neural preferences due to the meridional effect.²⁴ The resolution acuities were determined by varying the spatial frequency of the gratings with Bayesian adaptive psychophysical procedures. For this, MATLAB (www.mathworks.com) and Psychophysics Toolbox (www.psychtoolbox.org) were used to present the stimuli on a calibrated CRT monitor 2.6 m away from the subject. The subject's task was to identify the orientation of the gratings in a two-alternative forced choice paradigm, and respond with the corresponding key on a keypad. If the stimulus could not be resolved by the subject, the subject was instructed to guess. A guess rate of 50% and a lapse rate of 5% were set. To ensure that the subject was aware of the stimulus presentation, a sound cue was played at the start of each trial. The subjects did not receive feedback about whether they were responding right or wrong. The acuity was determined in 40 trials, and each grating stimulus was presented for 500 ms. Thresholds with a standard deviation >0.10 logMAR were retaken and the average acuity values were used for further analysis. All the measurements were repeated at least three times, and frequent breaks were given in order to avoid fatigue. To ensure that the procedure was understood, a test round was performed before the beginning of the actual experiment. The whole procedure with four conditions took almost 6 h per subject to perform (spread out during 2 days).

Results

The effect of the sign of defocus on peripheral vision was investigated under the four conditions shown in *Table 1*, with or without CA and HOA present. The resulting low-contrast resolution acuity for different amounts of peripheral defocus is presented individually for the nine subjects in *Figure 1*, with the different colours denoting the four different conditions according to *Table 1*.

In *Figure 1*, the defocus values are the actual peripheral defocus experienced by the eye as measured by the wavefront sensor of the AO system. As expected, best resolution acuity was achieved with minimum defocus for all conditions of optical correction. It is also evident that the rate of reduced vision with increasing defocus varies between the four different conditions, especially for the non-emmetropic subjects (i.e. s1, s3, s7, s8 and s9). The variation is larger for negative defocus, which tends to show a flatter profile for the condition with lowest correction (peripheral BSC correction, marked in yellow) and it becomes more alike that of positive defocus as the optical errors are corrected (Peripheral BSC + HOA correction, marked in black). This means that a subject like s1 shows better peripheral resolution acuity for negative defocus than for the same amount of positive defocus when the natural HOA and CA are present. To further analyse the rate of reduced vision with defocus, the MATLAB Curve Fitting Toolbox (www.mathworks.com) was used to least-square-fit the data in a V-shaped curve and to calculate the slopes for positive and negative defocus separately. *Figure 1* also presents the results of this fit as solid lines. Spurious resolution occurred for one of the subjects (*Figure 1*, s3, star data points with acuities better than the cut-off frequency of the theoretical MTF curve for -4 D of defocus), thus these data were not taken into consideration for the calculation of the slopes. A difference in the rate of reduced vision between positive and negative defocus (i.e. between the two slopes of the V-shaped curve in *Figure 1*) means that a subject is experiencing an asymmetry to peripheral defocus. *Table 2* lists the corresponding slopes, the average of the absolute values of the sum (AVS) of positive and negative defocus slopes and the average of the sum (AVS2) of positive and negative defocus slopes for each condition.

Figure 1 and *Table 2* show that peripheral resolution varied with defocus similarly for white and green light when the natural HOA were present. On average, the asymmetry for white and green light was 0.081 and 0.063 logMAR/D respectively. A Wilcoxon paired signed rank test ($T_+ = 10 > T_{0.05(2),9}$, $0.10 < p\text{-value} < 0.20$) on the absolute sums of positive and negative defocus for conditions (a) and (b) of all subjects in *Table 2* showed that our first null hypothesis, that the asymmetry is not affected by the CA of the eye, cannot be rejected. Furthermore, t-tests

performed on the slopes showed that when natural HOA were present: (1) there was a statistically significant difference ($p\text{-value} < 0.05$) between the slopes for negative and positive defocus for both green and white light for all subjects, (2) four of the subjects showed no statistically significant difference ($p\text{-value} > 0.05$) between the negative defocus slope for white light and the negative defocus slope for green light, and (3) there was no statistically significant difference ($p\text{-value} > 0.05$) between the positive defocus slope for white light and the positive defocus slope for green light for eight out of the nine subjects. These facts indicate that all subjects remained asymmetric after CA elimination, and that CA had no significant effect on the asymmetry. With adaptive optics correction for HOA, however, the subjects showed a more symmetric reduction in vision under positive and negative defocus with the sensitivity to negative (hypermetropic) defocus being affected the most by the HOA. After HOA correction the AVS was 0.021 logMAR/D for white light and 0.031 logMAR/D for green light. A Wilcoxon paired signed rank test ($T_+ = 0 < T_{0.05(2),9}$, $0.001 < p\text{-value} < 0.005$) on the absolute sums of positive and negative defocus for condition (a) and (c) of all subjects in *Table 2* showed that our second null hypothesis, that the asymmetry is not affected by the HOA of the eye, can be rejected. Thus, we can conclude that the asymmetry to peripheral defocus is mainly caused by the monochromatic HOA of the eye.

Discussion

This study investigates the effect of negative and positive defocus in peripheral vision with and without the off-axis aberrations present. In white light conditions with peripheral BSC correction (condition a), all the subjects showed asymmetric profiles with an AVS of 0.081 logMAR/D, being less sensitive to hypermetropic defocus. Similar asymmetric profiles have been found in foveal vision for myopic subjects by Guo *et al.*¹⁶ and Radhakrishnan *et al.*¹⁵ In the periphery, these asymmetric profiles are in agreement with Rosen *et al.*¹⁷ who also found asymmetries to the sign of defocus for both emmetropes and myopes.

The psychophysical test was performed successfully by all participants, and their cooperation was exceptional. The AO system performed very well throughout the procedure, and the acquired HOA correction was more than adequate (judging from the extracted Zernike coefficients). *Figure 2* shows an example of the monochromatic Modulation Transfer Function (MTF) curves of subject s5 for all four conditions when the subject was corrected for peripheral defocus and astigmatism i.e. no defocus induced. All subjects had clearly better image quality when the AO system was running and correcting the HOA of the eye. In addition, the monochromatic image quality was not affected by

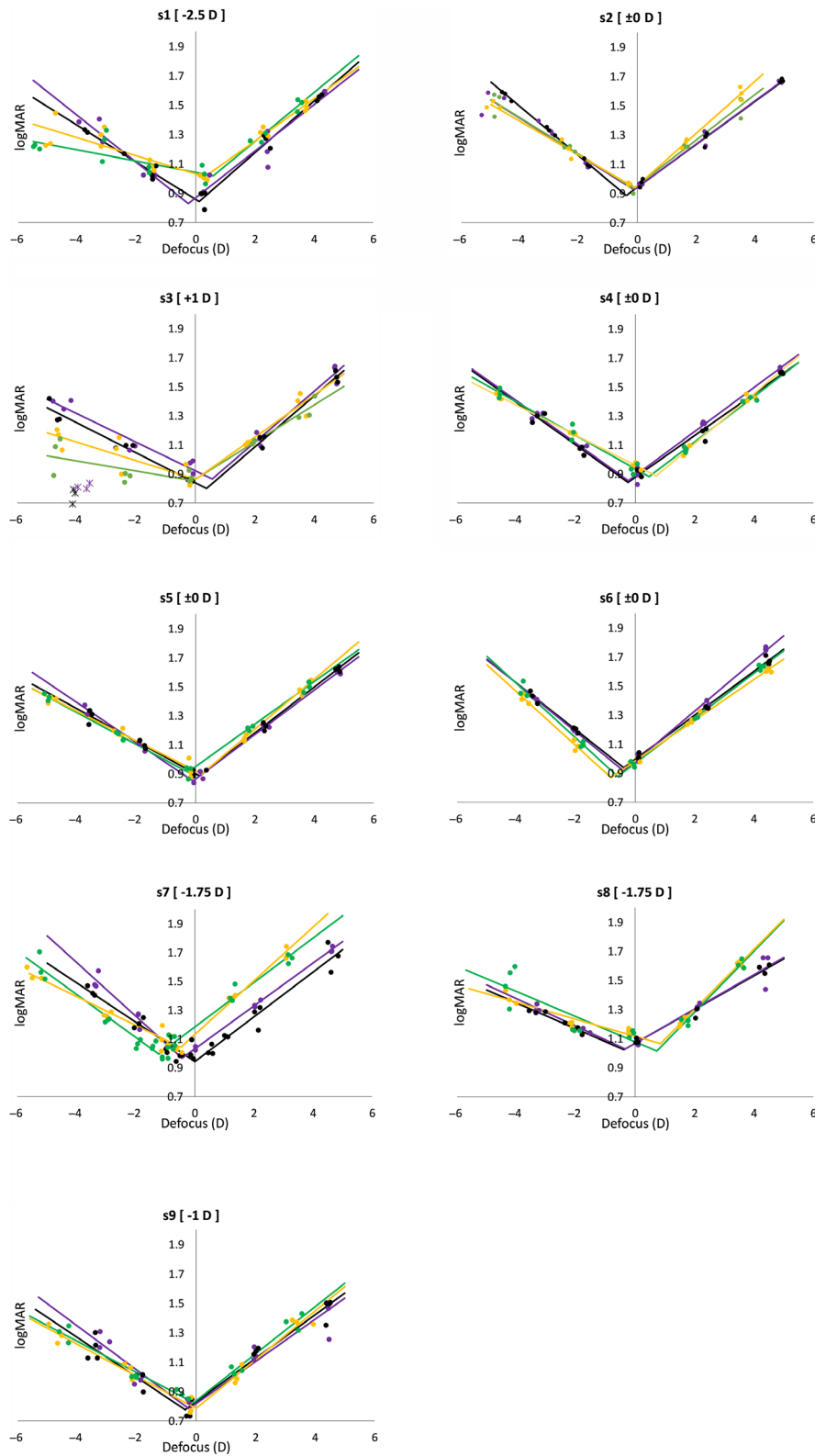


Figure 1. Peripheral low contrast (10%) resolution grating acuity in logMAR plotted against defocus in dioptres. Each graph represents one subject. The four conditions under which the experiments were performed are presented by the different colours and are summarised in *Table 1*. Spurious resolution that occurred for s3 is presented with the star data points.

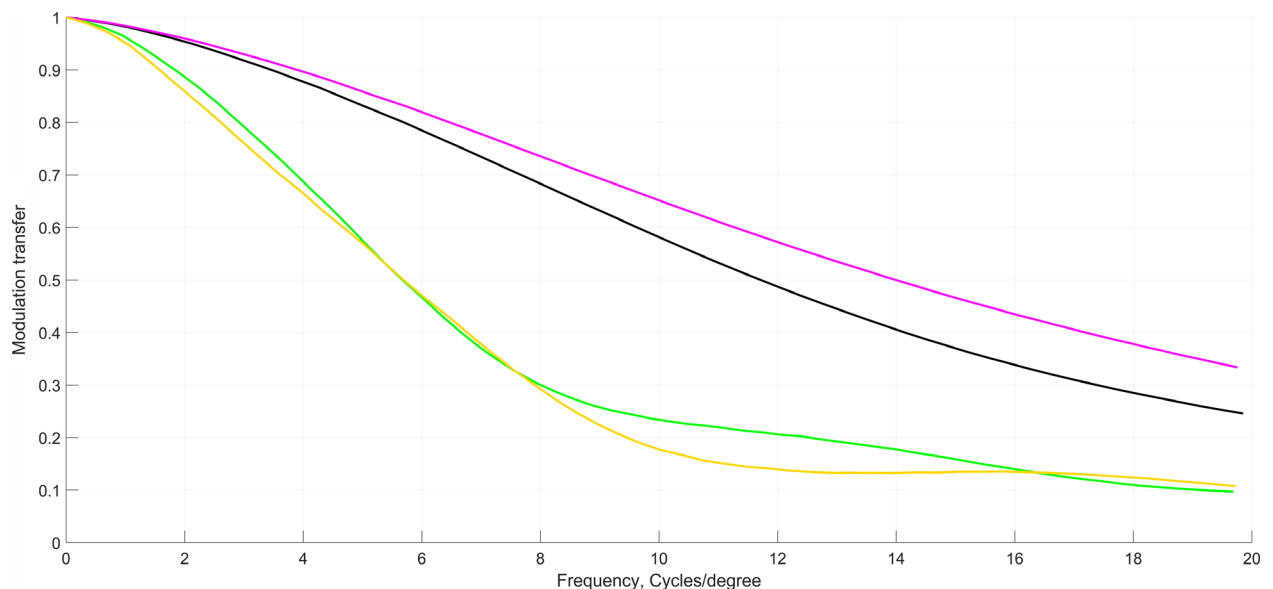
Table 2. The result of low-contrast (10%) resolution grating acuity tests in 20° nasal visual field expressed in slopes (logMAR/D)

[habitual refraction, age, pupil diameter]	a) White light BSC correction		b) Green light BSC correction		c) White light BSC + HOA correction		d) Green light BSC + HOA correction	
	Negative defocus	Positive defocus	Negative Defocus	Positive Defocus	Negative Defocus	Positive Defocus	Negative Defocus	Positive Defocus
s1 [-2.50 D, 39 years, 5.8 mm]	-0.06	0.14	-0.04	0.17	-0.16	0.16	-0.13	0.18
s2 [\pm 0 D, 25 years, 5.3 mm]	-0.12	0.18	-0.12	0.16	-0.13	0.15	-0.17	0.15
s3 [+1.00 D, 46 years, 3.7 mm]	-0.06	0.15	-0.03	0.13	-0.10	0.18	-0.10	0.18
s4 [\pm 0 D, 32 years, 5.0 mm]	-0.10	0.18	-0.11	0.16	-0.15	0.15	-0.15	0.14
s5 [\pm 0 D, 28 years, 4.7 mm]	-0.10	0.17	-0.11	0.15	-0.14	0.15	-0.11	0.16
s6 [\pm 0 D, 28 years, 5.7 mm]	-0.19	0.14	-0.19	0.15	-0.17	0.17	-0.16	0.15
s7 [-1.75 D, 33 years, 5.9 mm]	-0.10	0.19	-0.15	0.15	-0.19	0.15	-0.14	0.16
s8 [-1.75 D, 26 years, 4.2 mm]	-0.06	0.21	-0.09	0.21	-0.09	0.12	-0.09	0.12
s9 [-1.00 D, 25 years, 3.8 mm]	-0.11	0.17	-0.11	0.16	-0.15	0.14	-0.14	0.15
Average Slopes {logMAR/D}	-0.10	0.17	-0.11	0.16	-0.14	0.15	-0.13	0.15
AVS {logMAR/D}	0.081		0.063		0.021		0.031	
AVS2 {logMAR/D}	0.070		0.054		0.010		0.022	

Each row represents one subject with the subject's foveal refraction (in dioptres), age (in years) and average pupil diameter (in mm) in the brackets. Each column represents one condition, each sub-column represents the slopes as well as the average of the slopes for positive and negative defocus for each condition. AVS refers to the average of the absolute values of the sum of positive and negative defocus slopes and AVS2 refers to the average of the sum of positive and negative defocus slopes. Bold values indicates most important numbers.

using the filter and narrowing down the spectrum of the light (conditions b, d with CA elimination). We can thereby conclude that the subjects did not accommodate differently when the green filter was introduced in the AO system, neither when the AO system was off nor when it was running in closed loop. One of the challenging parts of the experiment was to find the best peripheral trial lens

correction for some of the subjects, which reflects the difficulty of defining a fast and accurate metric for peripheral refraction. For practical reasons, the trial lens correction was simply chosen based on the second order Zernike coefficients, ignoring the HOA. This approach led to a difference in the tested defocus values between the conditions with and without HOA correction for some subjects, but

**Figure 2.** Peripheral monochromatic Modulation Transfer Function (MTF) curves for subject s5 when no defocus was induced. The four conditions under which the experiments were performed are represented by the different colours and are summarised in Table 1.

did not affect the measured slopes. Also, a few subjects had large pupils and large aberrations in the periphery. Thus, the deformable mirror had to obtain large strokes when the AO system was running in close loop in order to correct the HOA. For the safety of the mirror, when the strokes were too large, we had to stop the experiment, flatten the mirror and restart this specific set.

Hypothesis 1

The Wilcoxon test on the absolute sums of positive and negative defocus for conditions (a) and (b) showed that our first null hypothesis, that the asymmetry is not affected by the CA of the eye, cannot be rejected. Furthermore, our measurements showed that the asymmetry remained and was very similar for white and green light when the natural HOA were present. We therefore concluded that the asymmetry is not mainly caused by the ocular CA.

Various animal studies suggest that wavelength-dependent defocus caused by the longitudinal chromatic aberration (LCA) of the eye can trigger or stop eye growth. Experiments in different animal models show that eyes treated with red light grew too long to compensate for the hypermetropic defocus and as a result they became myopic. Similarly, eyes treated with blue light showed less axial elongation.²⁸ This indicates a strong effect of LCA on animals' eyes. We did not test red and blue light separately in this study, but our results do not contradict the previous findings in animals.

Hypothesis 2

The Wilcoxon paired signed rank test on the absolute sums of positive and negative defocus for conditions (a) and (c) showed that our second null hypothesis, that the asymmetry is not affected by the HOA of the eye, can be rejected. We therefore conclude that the ocular HOA play a major role in the asymmetric sensitivity to peripheral defocus and that the effect of imposing negative and positive defocus is more symmetric when HOA are corrected. This finding supports the hypothesis of the aforementioned study by Rosen *et al.*¹⁷ that HOA increase the depth of focus also in the periphery.

Importance for myopia research

In the foveal study by Radhakrishnan *et al.* the asymmetry to defocus was only found for the myopic subjects and not for the emmetropes (although that study may suffer from pupil size artefacts due to magnification between the spectacle plane, the artificial pupils and the entrance pupil)

whereas Guo *et al.* showed asymmetric behaviour also for the emmetropic subject.^{15,16} By averaging the AVS values separately for myopes (mAVS) and emmetropes (eAVS) in the current study, it can be seen that the group of myopic subjects tended to be more asymmetric than the group of emmetropic subjects under all conditions, although the difference was not statistically significant. When the HOA were present, the mAVS and the eAVS values were 0.095 logMAR/D and 0.065 logMAR/D for white light, and 0.075 logMAR/D and 0.043 logMAR/D for green light respectively. A larger asymmetry for myopes would suggest a more asymmetric depth of focus, which could be caused by HOA. Some previous studies found no correlation between foveal HOA and refractive error,^{29–31} whereas others report a correlation between HOA and myopia.^{32–36} Additionally, in a recent review on peripheral optical errors, myopes had slightly worse image quality than emmetropes in the 20° visual field.³⁷ Further studies with larger sample size are needed to see whether myopes are less symmetric than emmetropes in their sensitivity to peripheral defocus. Either way the asymmetry can be important for myopia control. For example, interventions that compensate for the HOA of the peripheral eye and reduce the peripheral depth of focus could be more efficient in slowing myopia progression.

Acknowledgements

This research project was supported by the MyFUN project that receives funding from The European Union's Horizon 2020 research and innovation programme under the Marie Skłodowska-Curie grant agreement No 675137.

Conflict of interest

The authors report no conflicts of interest and have no proprietary interest in any of the materials mentioned.

References

1. World Health Organization. *The Impact of Myopia and High Myopia: Global Scientific Meeting on Myopia*. World Health Organization - Brien Holden Vision Institute, 2015.
2. Flitcroft DI. The complex interactions of retinal, optical and environmental factors in myopia aetiology. *Prog Retin Eye Res* 2012; 31: 622–660.
3. Goldschmidt E & Jacobsen N. Genetic and environmental effects on myopia development and progression. *Eye* 2014; 28: 126–133.
4. Winawer J & Wallman J. Homeostasis of eye growth and the question of myopia. *Neuron* 2004; 43: 447–468.
5. Smith EL, Kee CS, Ramamirtham R, Qiao-Grider Y & Hung LF. Peripheral vision can influence eye growth and refractive

- development in infant monkeys. *Invest Ophthalmol Vis Sci* 2005; 46: 3965–3972.
6. Benavente-Pérez A, Nour A & Troilo D. Axial eye growth and refractive error development can be modified by exposing the peripheral retina to relative myopic or hyperopic defocus. *Invest Ophthalmol Vis Sci* 2014; 55: 6765–6773.
 7. Smith EL, Hung LF & Arumugam B. Visual regulation of refractive development: Insights from animal studies. *Eye* 2014; 28: 180–188.
 8. Huang J, Weng D, Wang Q *et al.* Efficacy comparison of 16 interventions for myopia control in children: A network meta-analysis. *Ophthalmology* 2016; 123: 697–708.
 9. Curcio CA, Sloan KR, Kalina RE & Hendrickson AE. Human photoreceptor topography. *J Comp Neurol* 1990; 523: 497–523.
 10. Lundström L, Gustafsson J & Unsbo P. Vision evaluation of eccentric refractive correction. *Optom Vis Sci* 2007; 84: 1046–1052.
 11. Lundström L, Manzanera S, Prieto PM *et al.* Effect of optical correction and remaining aberrations on peripheral resolution acuity in the human eye. *Opt Express* 2007; 15: 12654.
 12. Anderson RS, McDowell DR & Ennis FA. Effect of localized defocus on detection thresholds for different sized targets in the fovea and periphery. *Acta Ophthalmol Scand* 2001; 79: 60–63.
 13. Wang YZ, Thibos LN & Bradley A. Effects of refractive error on detection acuity and resolution acuity in peripheral vision. *Invest Ophthalmol Vis Sci* 1997; 38: 2134–2143.
 14. Rosén R, Lundström L & Unsbo P. Influence of optical defocus on peripheral vision. *Invest Ophthalmol Vis Sci* 2011; 52: 318–323.
 15. Radhakrishnan H, Pardhan S, Calver RI & O'Leary DJ. Unequal reduction in visual acuity with positive and negative defocusing lenses in myopes. *Optom Vis Sci* 2004; 81: 14–17.
 16. Guo H, Atchison DA & Birt BJ. Changes in through-focus spatial visual performance with adaptive optics correction of monochromatic aberrations. *Vision Res* 2008; 48: 1804–1811.
 17. Rosén R, Lundström L & Unsbo P. Sign-dependent sensitivity to peripheral defocus for myopes due to aberrations. *Invest Ophthalmol Vis Sci* 2012; 53: 7176–7182.
 18. Rucker FJ & Wallman J. Chick eyes compensate for chromatic simulations of hyperopic and myopic defocus: Evidence that the eye uses longitudinal chromatic aberration to guide eye-growth. *Vision Res* 2009; 49: 1775–1783.
 19. Rynders MC, Navarro R & Losada MA. Objective measurement of the off-axis longitudinal chromatic aberration in the human eye. *Vision Res* 1998; 38: 513–522.
 20. Jaeken B, Lundström L & Artal P. Peripheral aberrations in the human eye for different wavelengths: off-axis chromatic aberration. *J Opt Soc Am A* 2011; 28: 1871.
 21. Lundström L & Rosén R. Peripheral aberrations. In: Artal P, (ed), *Handbook of Visual Optics, Volume One: Fundamentals and Eye Optics*, London: Taylor & Francis, 2017; pp. 313–335.
 22. Winter S, Sabesan R, Tiruveedhula P *et al.* Transverse chromatic aberration across the visual field of the human eye. *J Vis* 2016; 16: 9.
 23. Rosén R, Lundström L & Unsbo P. Adaptive optics for peripheral vision. *J Mod Opt* 2012; 59: 1064–1070.
 24. Venkataraman AP, Winter S, Rosén R & Lundström L. Choice of grating orientation for evaluation of peripheral Vision. *Optom Vis Sci* 2016; 93: 567–574.
 25. Venkataraman AP, Papadogiannis P, Romashchenko D, Winter S, Unsbo P & Lundström L. Peripheral resolution and contrast sensitivity: effects of monochromatic and chromatic aberrations. *J Opt Soc Am A* 2019; 36: B52.
 26. Thibos LN, Hong X, Bradley A & Applegate RA. Accuracy and precision of objective refraction from wavefront aberrations. *J Vis* 2004; 4: 329–351.
 27. Hartwig A, Murray IJ & Radhakrishnan H. Peripheral aberration measurements: Elliptical pupil transformation and variations in horizontal coma across the visual field. *Clin Exp Optom* 2011; 94: 443–451.
 28. Rucker F. Monochromatic and white light and the regulation of eye growth. *Exp Eye Res* 2019; 184: 172–182.
 29. Porter J, Guirao A, Cox IG & Williams DR. Monochromatic aberrations of the human eye. *J Opt Soc Am A Opt Image Sci Vis* 2001; 18: 1793–1803.
 30. Cheng X, Bradley A, Hong X & Thibos LN. Relationship between refractive error and monochromatic aberrations of the eye. *Optom Vis Sci* 2003; 80: 43–49.
 31. Little JA, McCullough SJ, Breslin KMM & Saunders KJ. Higher order ocular aberrations and their relation to refractive error and ocular biometry in children. *Invest Ophthalmol Vis Sci* 2014; 55: 4791–4800.
 32. Lau JK, Vincent SJ, Collins MJ, Cheung SW & Cho P. Ocular higher-order aberrations and axial eye growth in young Hong Kong children. *Sci Rep* 2018; 8: 2–11.
 33. Hiraoka T, Kotsuka J, Kakita T, Okamoto F & Oshika T. Relationship between higher-order wavefront aberrations and natural progression of myopia in schoolchildren. *Sci Rep* 2017; 7: 1–9.
 34. Zhang N, Yang X-B, Zhang W-Q *et al.* Relationship between higher-order aberrations and myopia progression in schoolchildren: A retrospective study. *Int J Ophthalmol* 2013; 6: 295–299.
 35. Karimian F, Feizi S & Doozande A. Higher-order aberrations in myopic eyes. *J Ophthalmic Vis Res* 2010; 5: 3–9.
 36. Buehren T, Collins MJ & Carney LG. Near work induced wavefront aberrations in myopia. *Vision Res* 2005; 45: 1297–1312.
 37. Romashchenko D, Rosén R & Lundström L. Peripheral refraction and higher order aberrations. *Clin Exp Optom* 2020; 103: 1–9.